EXPLORATION OF MEMBRANE-BASED DEHUMIDIFICATION SYSTEM TO IMPROVE THE ENERGY EFFICIENCY OF KILN-DRYING PROCESSES: PART I FACTORS THAT AFFECT MOISTURE REMOVAL EFFICIENCY

Nasim Alikhani†

Graduate Research Assistant
E-mail: nasim.alikhani@maine.edu

*Ling Li**†

Assistant Professor of Sustainable Bioenergy Systems
School of Forest Resources
University of Maine
Orono, ME 04469
E-mail: ling.li@maine.edu

Jinwu Wang

Research Forest Products Technologist
USDA Forest Service, Forest Products Laboratory
Madison, WI 53726
E-mail: jinwu.wang@usda.gov

Darien Dewar

Undergraduate Research Assistant
College of Engineering
Valparaiso University
Valparaiso, IN 46383
E-mail: darien.dewar@valpo.edu

Mehdi Tajvidi†

Associate Professor of Renewable Nanomaterials
School of Forest Resources
University of Maine
Orono, ME 04469
E-mail: mehdi.tajvidi@maine.edu

(Received March 2020)

Abstract. Green wood drying through a steam kiln-drying technology is an energy-demanding process. This process consumes a large amount of energy to evaporate water from wood and discharge it to the atmosphere through venting. The thermal energy loss from the venting of dry kilns takes up to 20% of total energy consumed by the whole wood-drying operation because a considerably large amount of thermal energy is stored in exhaust air. Harvesting and reusing such waste thermal energy would improve the energy efficiency of the kiln-drying process. Advanced moisture-selective membranes have been used to dehydrate humid air or gas steam because of the advantages of low energy requirements, simplicity of operation, and high specificity. However, the application of the membrane in wood-drying processes has not been addressed. Therefore, this study aimed to investigate the feasibility of using a moisture-selective membrane system to dehydrate the warm moist exhaust air to achieve an energy-saving purpose. The membrane

* Corresponding author
† SWST member

Wood and Fiber Science, 52(3), 2020, pp. 313-325
https://doi.org/10.22382/wfs-2020-029

material was polydimethylsiloxane (PDMS) with high water vapor permeability. A small membrane-based dehumidification system was constructed to evaluate the effects of four factors (temperature, airflow rate, initial RH, and vacuum pressure) on the efficiency of moisture vapor removal. Statistical analysis in terms of response surface methodology was carried out. The major findings include 1) an increase in the temperature and vacuum pressure caused a significant increase in the efficiency of moisture vapor removal, 2) the initial RH had little influence on the efficiency of moisture vapor removal, 3) increasing the airflow rate had a negative impact on the efficiency of moisture vapor removal, and 4) the regression model can be used to predict the efficiency of moisture vapor removal. This PDMS membrane would be a possible solution for a predrying process at relatively low operation temperatures (<45°C), that is dehumidification process.

Keywords: Energy efficiency, kiln-drying processes, moisture selective membrane, thermal energy recovery system, waste thermal energy.

INTRODUCTION

Green wood usually has high MCs, a range being from 60% to 120% on a dry weight basis. The kiln-drying process is a key process in drying lumber/boards fast to reduce their MCs to the required final MCs for various applications. The conventional steam-drying kiln is the most commonly used kiln type in North America. In this particular process, steam is circulated in heating coils to heat air and spraying lines to adjust the RH of the air based on a specified drying schedule. Free water and bound water in wood evaporate into the air in the kiln. Gradually, the air becomes saturated with moisture and loses its drying power (Field and Long 2018). The humid and hot air is typically ventilated to the environment regularly. Because the air moisture-holding capacity increases exponentially with the temperature (Chadderton 1997), relatively cold and dry air is brought into the kiln to absorb the water vapor that is escaping from lumber. Although the kiln-drying process greatly decreases the time required to produce dry wood, it consumes a large amount of heat energy to lower the MC of wood (Simpson 1991). During the kiln-drying process, energy is consumed by several elements such as latent heat of evaporating water, heat loss from kiln structures (walls and doors), heat loss from venting air, and sensible heat to warm lumber, air, water, and kiln structures, most of which are irreversible. The heat loss can only be partially recovered through ventilation to serve an energy-saving purpose. It was reported that about 20% of heat energy loss in conventional dry kilns was ascribed to the ventilation of exhaust air (Garrahan 2008). There have been several energy recovery systems that have been applied to conventional dry kilns. One of them uses heat exchangers to capture the sensible heat of exhaust air and transfer it to the incoming fresh cold air. The efficiency of energy recovery of these systems varies with environmental conditions, for example the difference in temperature between the air inside the kiln and incoming fresh air in summer is less than that in winter. In addition, the RH of the incoming air is affected by environmental conditions as well, for example moist air in rainy/snowy days.

With the rapid development of membrane technology during recent decades, it has been shown that a type of moisture-selective membrane can effectively and efficiently remove moisture from the air. An example of this application is in certain air-conditioning units used in the Heating, Ventilation, and Air Conditioning (HVAC) system of buildings (Kneifel et al 2006; Elustondo et al 2009). Overall, membrane-based dehumidification systems have numerous advantages: less energy consumption because the moisture vapor is removed through diffusion without undergoing a phase change (ie moisture vapor at the permeate side), unlike the heat pump dehumidification system via condensation; simplicity in maintenance and operation; high selectivity; ease of scale-up; and low initial cost (Yang et al 2015; Zhao et al 2015; Liang and Chung 2018). The membrane dehumidification technology shows promising potential for the wood industry's need to reduce energy consumption. A hypothesis is that energy saving could be achieved when dry air is separated from the humid and hot exhaust air and the dry, hot air is rerouted back into the kiln,

thereby reducing the energy required to heat another cold air stream coming into the kilns from the environment, as shown in Fig 1.

To investigate the feasibility of using a moisture-selective membrane module to develop a closed energy recovery system that can improve the energy efficiency of the wood-drying process, a small laboratory unit was set up to study the effects of temperature, airflow rate, initial RH, and vacuum pressure on the moisture separation efficiency of the system.

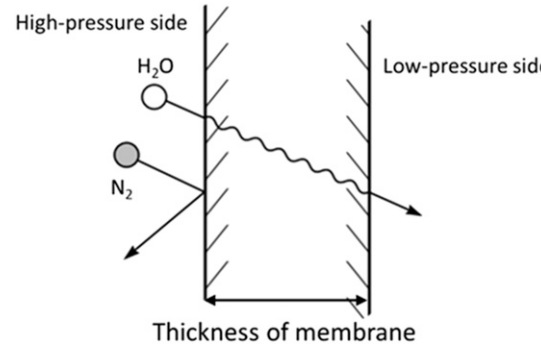

Figure 2. Gas separation mechanism of a dense polymer membrane (adapted from Baker 2012).

MATERIALS AND METHODS

Membrane Material

Water vapor separation mechanism of membranes. Water vapor in air can be separated by dense polymer-based membranes (Sijbesma et al 2008). Such dense membrane separates mixed gas components in terms of the differences in solubility and diffusivity of the components in the membrane material. A solution–diffusion process, as shown in Fig 2, which is driven by the difference in pressure between the two sides of the membrane, is briefly described in the following texts (Baker 2012):

1. Under applied high pressure, water vapor molecules in a gas mixture first are adsorbed on the membrane surface.
2. Then, the water vapor molecules diffuse through the thickness of the membrane, which is facilitated by the concentration gradient of water vapor (Fick's law); this generates a net flow toward the low-concentration side.
3. The water vapor molecules desorb at the low-pressure side of the membrane (ie the opposite side of the feed gas).

Selection of membrane material. Literature review reveals that many polymer-based membrane materials can be used for the removal of water vapor from air or gas streams, as seen in Fig 2 (Blume et al 1991; Wang et al 1992; Jia et al 1996, 1997; Mulder 1996; Metz et al 2005; Kneifel et al 2006; Phillip et al 2006; Montoya 2010; Wai Lin and Valera Lamas 2011; Bergmair et al 2012). Water vapor permeability and H_2O/N_2 selectivity are two primary parameters in selecting membranes for various applications. Considering medium-size to large-size

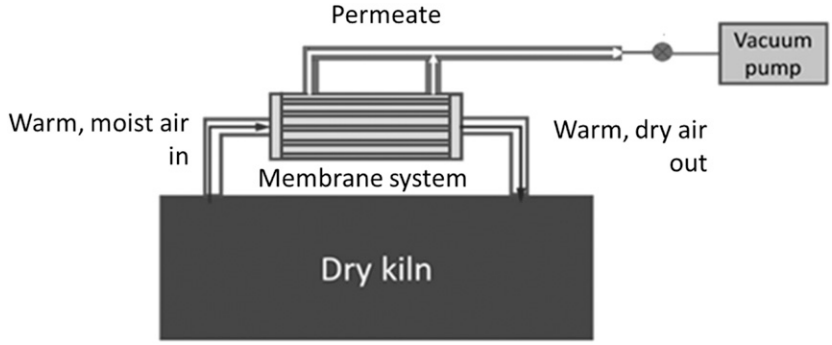

Figure 1. Schematic of a membrane-based energy recovery system being applied in dry kiln.

steam-drying kilns, large volumetric moisture vapor would be expelled from the vents regularly. It then requires that the membrane have a high water vapor permeability to quickly remove the excess water vapor in air. Likewise, the H_2O/N_2 selectivity should be high enough to effectively separate the moisture vapor from air.

In this study, a membrane material of polydimethylsiloxane (PDMS) was selected. A hollow fiber membrane module made of PDMS was purchased from PermSelect-MedArray Inc (Ann Arbor, MI, USA). Based on the fact sheet provided by the material supplier, the water vapor permeability is 36,000 Barrer ($1\ \text{Barrer} = 3.35 \times 10^{-16} \frac{\text{mol} \cdot \text{m}}{\text{m}^2 \cdot \text{s} \cdot \text{Pa}}$) and the H_2O/N_2 selectivity is 129, as shown in Fig 3. The supplier recommended operating the membrane module below 60°C to obtain the optimum result. However, considering that most softwood drying processes are conducted in a conventional temperature range, that is 45°C-82°C, the temperature limitation of the PDMS membrane should be overcome before targeting the application on the conventional kiln-drying processes. PDMS will be modified in future investigations, focusing on the operation capability of the system under higher temperatures. Nevertheless, this PDMS membrane would be a possible solution for a predrying process, that is dehumidification process. Also, the experimental results of the PDMS membrane obtained in this study will be used as a benchmark to compare with the modified PDMS membrane.

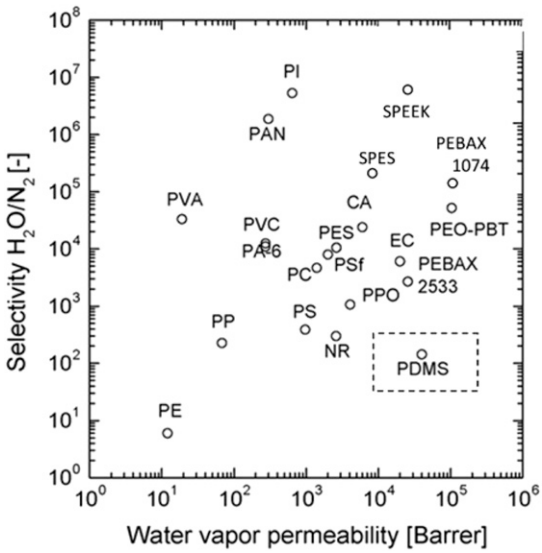

Figure 3. Water vapor permeability and H_2O/N_2 selectivity of various polymer-based membranes (Sijbesma et al 2008).

Experimental setup. A hollow fiber PDMS membrane module enclosing bundles of hollow fibers with a surface area of 1.0 m^2 (Fig 4[a]) was used for fabricating the dehumidification system because of the compact size. The SEM image (Fig 4[b]) shows the cross section of a single fiber with approximately 55-μm-thick wall. As illustrated in Fig 4 [c], the feed gas mixture flows in one end of the lumen of the fiber and exhausts from the other end. Most water vapor molecules permeate through the thickness of the PDMS fiber to the shell side, forming a cross-flow mode.

As shown in the schematic of a small-scale membrane dehumidification system (Fig 5), the membrane system was placed in a temperature- and RH-controlled environmental chamber. Humid air entered the membrane module through inlet 1. The airflow rate was controlled by an air blower and monitored by a mass/volume flowmeter. Humid air passed through the lumen of hollow fibers, and dehumidified air came out of outlet 2, which was collected in a closed airtight container for the measurement of RH and temperature. The temperature and RH of both humid air and dehumidified air were monitored and recorded with time at an interval of 10 s by temperature and humidity sensors and a data logging system. The moisture vapor that permeated through the wall of hollow fibers came out of outlet 3 and outlet 4 and expelled to the outside of the environmental chamber through a vacuum pump. The vacuum pump was equipped with a vacuum regulator and a moisture trap. Port 5 was blocked during the whole testing process.

The efficiency of water vapor removal is calculated using Eq 1:

$$\text{Efficiency}(\%) = \frac{(\text{RH}_{\text{in}} - \text{RH}_{\text{out}})}{\text{RH}_{\text{in}}} \times 100, \quad (1)$$

where RH_{in} is the initial RH of humid air entering inlet 1 (Fig 5) and RH_{out} is the RH of dehumidified

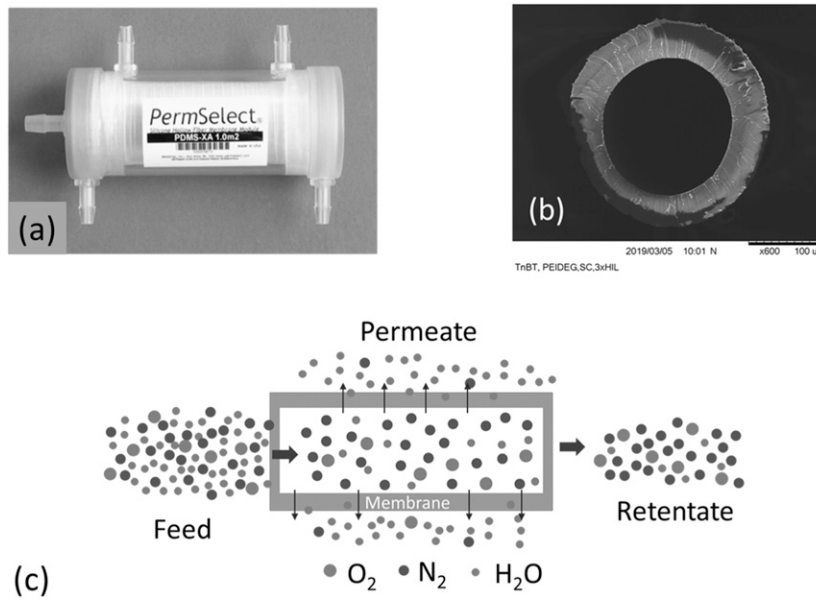

Figure 4. View of a hollow fiber polydimethylsiloxane membrane (surface area = 1 m^2) (a), a cross section of one single tube (b), and a schematic of gas separation (c).

air coming out of outlet 2 (Fig 5). It is worth noting that the RH_{out} was the value of the level-off stage when a steady state was reached, as shown in Fig 6.

Experimental Design

Selection of four factors. Four factors were investigated including temperature, airflow rate, RH, and vacuum pressure. Temperature (dry bulb), RH, and airflow rate were selected because they are three key parameters of the wood-drying process, which vary with the drying schedule of different wood species. Because a vacuum pump was used to generate a pressure difference between the two sides of the membrane in this study, vacuum pressure was chosen as a factor. Table 1 lists the four factors and three levels of each factor.

Temperatures of moist air were set in a low range of 25°C-45°C because of the temperature limitation of the environmental chamber used in the laboratory, and the maximum operating temperature for the airflow meter is 50°C. The levels of volumetric airflow rate were determined by the cross-sectional area of the inlet of the small PDMS membrane module, and air velocity commonly circulated in the kiln, for example 23 m/min for drying Douglas fir.

Response surface methodology (RSM). The RSM was used to design the experiment and analyze the data. RSM is a collection of mathematical and statistical techniques which is used to model and analyze problems in which a response of interest is influenced by several factors (Bezerra et al 2008; Vildozo et al 2010; Saldaña-Robles et al 2014). In this study, SPSS software (IBM SPSS statistics for Windows, version (2019)) was used to conduct the experimental design and statistical analysis. There were 29 testing combinations designed by using a Box–Behnken design model of RSM. Each testing combination was replicated three times, generating a total of 87 testing runs. The mean of three replicates was used in the statistical analysis.

After completing all the tests, the relationships of the response (ie efficiency of moisture vapor removal) with the four factors were displayed in

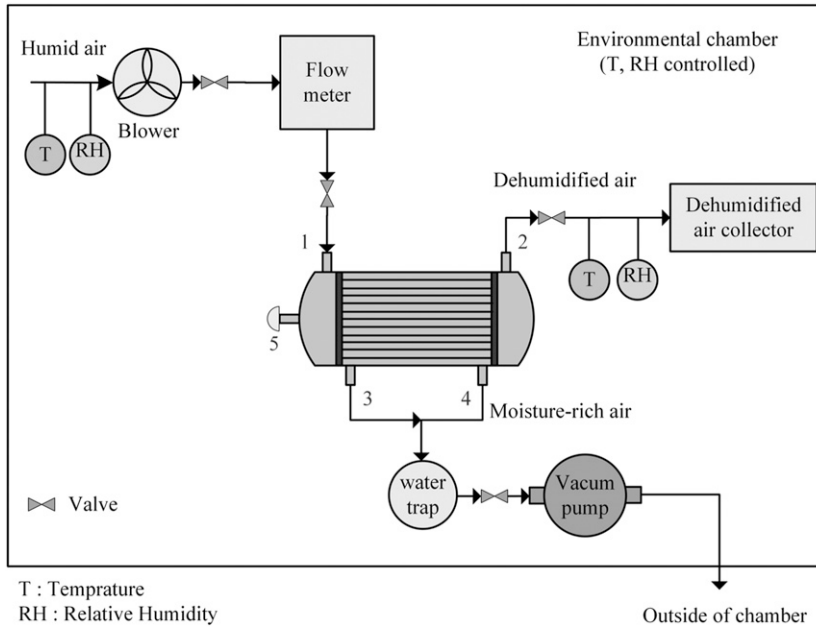

Figure 5. Schematic of a membrane dehumidification system.

the form of a response surface plot based on the calculated results using a regression model. Meanwhile, the analysis of variance (ANOVA) was conducted using the mean of three replicates for each testing combination.

Experiment of verification of regression model. To verify the regression model for the prediction of the efficiency of moisture vapor removal, a verification experiment was conducted at a temperature of 30°C, initial RH% of 70%, airflow rate of 700 cm^3/min, and vacuum pressure of 74.5 kPa. These parameters were randomly selected within the range of each variable listed in Table 1, but they were different from the values used for developing the regression model. The test was replicated three times. The mean value of three replicates was compared with the result predicted by the regression model.

RESULTS AND DISCUSSION

Reduction of RH with Time

The experimental results show that all the curves share the same trend so that only representative curves with testing conditions labeled are plotted in Fig 6. It shows that the RH of the dehumidified air at outlet 2 dropped quickly at the beginning (less than 5 min into the run), after the membrane system started working, and then reached a steady state to maintain a constant RH during the remaining testing period. Because the RH at outlet 2 could reach a constant in such a short time, the testing period was set to 20 min. The durability and lifetime of the membrane system were not addressed in this study.

Effects of Test Factors on Efficiency of Moisture Vapor Removal

Main effects of test factors. The main effects of the four factors are shown in Fig 7. The main effect of a specific factor was ploted as the other three factors were fixed at the medium level, as listed in Table 1. The results reveal that the efficiency of moisture vapor removal increased by approximately 75% with the increase in temperature from 25°C to 45°C and vacuum pressure from 68 kPa to 88 kPa, respectively. On the contrary, it decreased by approximately 25% with an increase in airflow rate from 600 cm^3/min to 1000 cm^3/min. Increasing

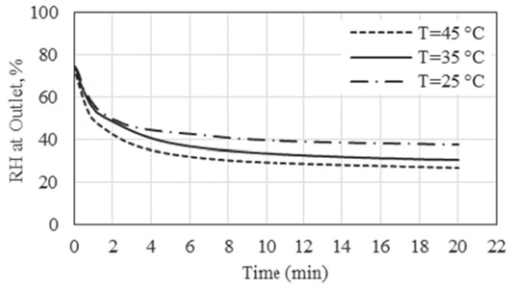

(a) Pressure = 78 kPa, Flow rate = 800 cm^3/min; RH = 75%;

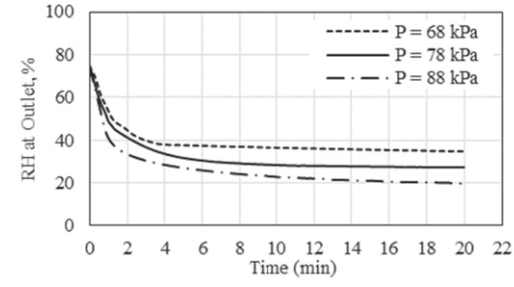

(b) Temperature=35°C, Flow rate = 800 cm^3/min, RH = 75%;

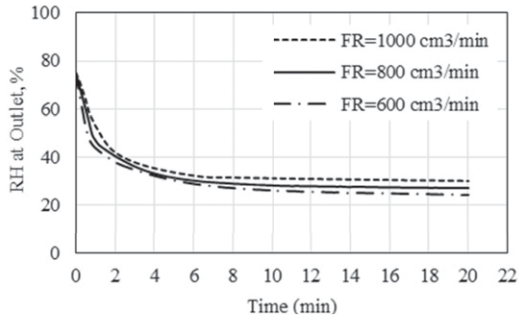

(c) Temperature=35°C, Pressure=78 kPa, RH = 75%

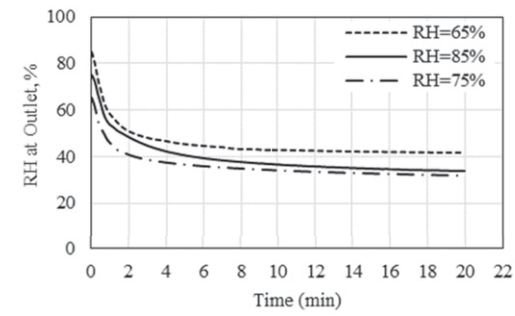

(d) Temperature=35°C, Flow rate = 800 cm^3/min, Pressure = 78 kPa

Figure 6. General curves of the reduction of RH at the outlet with time at representative testing conditions. (a) Pressure = 78 kPa, flow rate = 800 cm^3/min; RH = 75%. (b) Temperature = 35°C, flow rate = 800 cm^3/min, RH = 75%. (c) Temperature = 35°C, pressure = 78 kPa, RH = 75%. (d) Temperature = 35°C, flow rate = 800 cm^3/min, pressure = 78 kPa.

the initial RH from 65% to 85% had little effect on the efficiency of moisture vapor removal.

The influence of temperature on the moisture vapor removal may be explained by the difference in the kinetic energy of gas molecules at different temperatures. The kinetic energy of gas molecules at a high temperature is larger than that at a low temperature. The higher the temperature, the higher can be the mobility of moisture vapor molecules, increasing the number of such molecules adsorbed at the surface of the membrane.

Table 1. Factors and levels of each factor.

	Levels		
Factor	Low	Medium	High
Temperature (T), °C	25	35	45
Initial RH, %	65	75	85
Airflow rate (FR), cm^3/min	600	800	1000
Vacuum pressure, kPa	68	78	88

The impact of temperature on the moisture vapor permeance has not been widely investigated in studies regarding PDMS membranes, but in studies of other types of polymer-based membranes. Park et al (2013) revealed that the moisture vapor permeance of polyethyleneimine/polyether block amide composite hollow fiber membrane increased with temperature from 50°C, 70°C, and 90°C. Metz (2005) examined the influence of temperature on the permeability and selectivity of water vapor for poly(ethylene oxide)–poly(butylene terephthalate) block copolymers. They concluded that the permeability and selectivity for these block copolymers are temperature and structure dependent. However, because of the limitation of material supply, the permeability and selectivity of PDMS used in this study were not measured at different temperatures. They will be addressed in a future work. The high vacuum pressure, in turn, generates a large

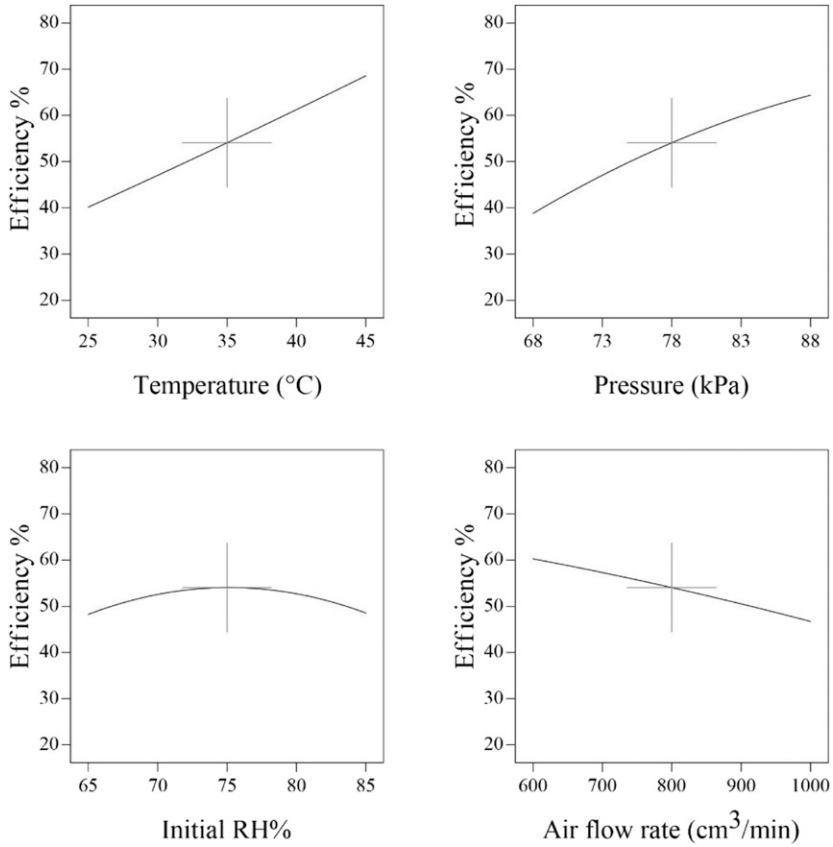

Figure 7. Main effects of the four factors on the efficiency of moisture vapor removal (the other three factors fixed at the medium level).

difference in pressure between the two sides of the membrane, driving the moisture vapor molecules to diffuse from the high- to the low-concentration side. Regarding the airflow rate, the negative impact caused by increasing its value is due to a reduced residence time of the water vapor molecules when traveling through the tube side of the membrane module. Therefore, less water vapor molecules were absorbed by the membrane.

Our results about the influence of vacuum pressure, airflow rate, and initial RH are in line with the water vapor removal results obtained from a PDMS/polyacrylonitrile hollow fiber membrane system (Liang and Chung 2018). In their study, the water vapor permeability of a thin PDMS layer (about 3.61 μm) was 13,335 Barrer. The efficiency of moisture vapor removal was approximately 50%, as the initial RH was in the range of 60-90%, and the vacuum pressure was about 98 kPa; 80% of moisture vapor was removed from the moist air as the feed flow rate was low to 400 cm^3/min, and only 50% of moisture vapor was separated as the feed flow rate was high to 1000 cm^3/min. The impact of temperature was not addressed in their study. The results presented in this study and literature indicate that to achieve a better performance of moisture removal, the desired opearting settings of the membrane system are high temperature, high vacuum pressure, and low airflow rate.

Interaction Effects of Test Factors

The interaction effects of two of four factors on the efficiency of moisture vapor removal are

plotted in terms of a response surface contour plot, as seen in Fig 8(a)-(f). In each plot, the contour curves show the efficiency of water vapor removal at various levels of temperature, vacuum pressure, RH, and airflow rate predicted by a simplified regression model (adj. $R^2 = 0.947$), which is discussed in the subsection of analysis of ANOVA. Each of these plots presents the effect

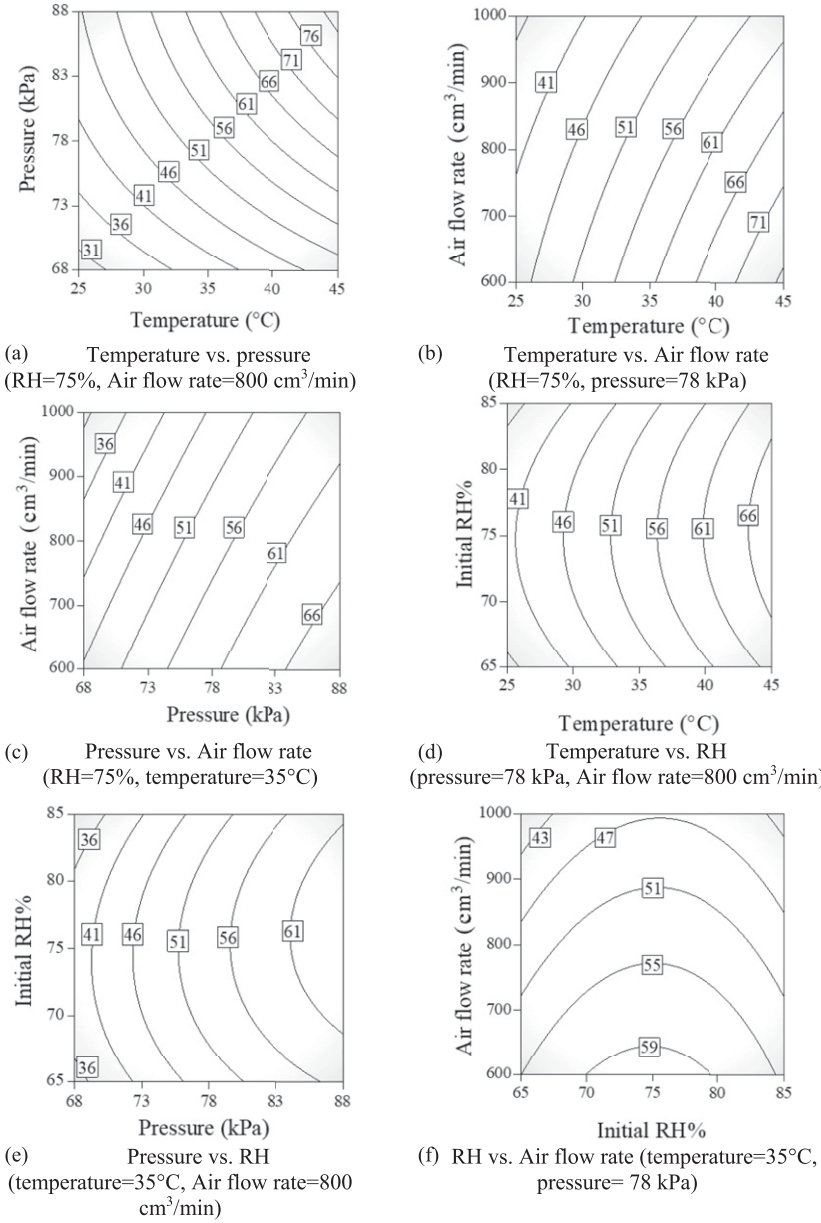

(a) Temperature vs. pressure (RH=75%, Air flow rate=800 cm^3/min)

(b) Temperature vs. Air flow rate (RH=75%, pressure=78 kPa)

(c) Pressure vs. Air flow rate (RH=75%, temperature=35°C)

(d) Temperature vs. RH (pressure=78 kPa, Air flow rate=800 cm^3/min)

(e) Pressure vs. RH (temperature=35°C, Air flow rate=800 cm^3/min)

(f) RH vs. Air flow rate (temperature=35°C, pressure= 78 kPa)

Figure 8. Effects of the interactions of between two factors on the efficiency of moisture vapor removal (the other two factors fixed at the medium level). (a) Temperature vs pressure (RH = 75%, airflow rate = 800 cm^3/min). (b) Temperature vs airflow rate (RH = 75%, pressure = 78 kPa). (c) Pressure vs airflow rate (RH = 75%, temperature = 35°C). (d): Temperature vs RH (pressure = 78 kPa, airflow rate = 800 cm^3/min). (e) Pressure vs RH (temperature = 35°C, airflow rate = 800 cm^3/min). (f) RH vs airflow rate (temperature = 35°C, pressure = 78 kPa).

of two factors on the efficiency. The remaining two factors were kept constant at their medium level (see Table 1).

The contour plot in Fig 8(a) provides information about the trend of the efficiency of water vapor removal as a function of temperature and vacuum pressure. The constant initial RH and airflow rate were 75% and 800 cm^3/min, respectively. It reveals, for instance, that the increase in temperature from 25°C to 45°C led to an increase in efficiency from approximately 30% to 50% at a low–vacuum pressure level of 68 kPa. At 45°C, if the vacuum pressure decreases from 88 kPa to 68 kPa, the efficiency decreases from approximately 82% to 50%. The interaction of temperature and vacuum pressure can be beneficial in the membrane system design by using a vacuum pump with a variable speed drive to reduce the noticeable energy consumption of continuously running the pump. For example during the drying process, the water vapor release rate, defined as the mass of water vapor per hour, decreases as the MC of lumber is below the Fiber Saturation Point (FSP) of lumber, which takes place at the last few steps of the drying schedule. In this situation, the membrane system can be operated at a relatively low vacuum pressure but can be maintained at an acceptable efficiency of water vapor removal.

Figure 8(b) shows the contour plot of efficiency as a function of temperature and airflow rate at a constant vacuum pressure of 78 kPa and initial RH of 75%. The plot shows a decrease in the efficiency of moisture vapor removal from approximately 44% to 35% as a consequence of an increase in the flow rate from 600 cm^3/min to 1000 cm^3/min at a constant temperature level of 25°C. At a high temperature of 45°C, increasing the airflow rate from 600 cm^3/min to 1000 cm^3/min results in a decrease in the efficiency of moisture vapor removal from approximately 76% to 58%. This indicates that temperature influences the mobility of gas molecules at any level of airflow rate.

Figure 8(c) shows the contour plot of efficiency as a function of pressure and airflow rate at a constant temperature of 35°C and initial RH of 75%. The plot shows a decrease in the efficiency of moisture vapor removal from approximately 45% to 30% as a result of increase in the flow rate from 600 cm^3/min to 1000 cm^3/min at a constant vacuum pressure of 68 kPa. As a result of a high vacuum pressure of 88 kPa, a decrease in the efficiency of moisture vapor removal from approximately 70% to 58% is observed.

The contour plot in Fig 8(d) provides information about the trend of the efficiency of moisture vapor removal as a function of temperature and initial RH when the vacuum pressure and airflow rate are set to 78 kPa and 800 cm^3/min, respectively. It can be observed that altering the initial RH does not significantly affect the efficiency of moisture removal at any temperature level. For instance, the difference in the efficiency of moisture vapor removal is approximately 4% as increasing RH from 65% to 85% at a temperature level of 35°C. This similar trend is observed in Fig 8(e) and (f), which show the interaction effects of pressure and initial RH and airflow rate and initial RH on the efficiency of moisture vapor removal.

ANOVA and a Regression Model of Efficiency of Moisture Vapor Removal

ANOVA, which is based on the mean values of 29 testing runs with three repetitions for each run, is illustrated in Table 2. The statistical significance of each factor and their interactions is denoted by p-value, the significance of which is 0.05. As shown in Table 2, the significant factors (p-value < 0.0001) include temperature, vacuum pressure, and airflow rate. However, initial RH (p-value $= 0.89$) is not statistically significant for the efficiency of moisture vapor removal. In addition, the interaction of temperature and vacuum pressure (p-value $= 0.0273$) is statistically significant for the efficiency of moisture vapor removal.

According to ANOVA, a quadratic regression model was developed. The regression model shown in Eq 2 is a simplified model by removing the items that have a p-value > 0.05 in Table 2. The adjusted R^2 value is 0.947. This regression

Table 2. Analysis of variance of test variables and their interactions.

Source	Sum of squares	D*f*	Mean square	*f*-value	*p*-value > *F*	Significance
Model	5297.53	14	378.40	28.41	<0.0001	*
T	2424.05	1	2424.05	182.01	<0.0001	*
P	1962.48	1	1962.48	147.35	<0.0001	*
RH	0.27	1	0.27	0.020	0.8887	—
FR	551.19	1	551.19	41.39	<0.0001	*
$T \times P$	80.88	1	80.88	6.07	0.0273	*
$T \times$ RH	0.99	1	0.99	0.074	0.7891	—
$T \times$ FR	18.53	1	18.53	1.39	0.2578	—
$P \times$ RH	8.40	1	8.40	0.63	0.4402	—
$P \times$ FR	9.01	1	9.01	0.68	0.4245	—
RH × FR	0.92	1	0.92	0.069	0.7965	—
T^2	0.54	1	0.54	0.041	0.8432	—
P^2	40.28	1	40.28	3.02	0.1040	—
RH^2	207.93	1	207.93	15.61	0.0014	*
FR^2	2.00	1	2.00	0.15	0.7040	—
Residual	186.46	14	13.32	—	—	—
Lack of fit	166.24	10	16.62	3.29	0.1312	—
Pure error	20.21	4	5.05	—	—	—
Cor total	5483.99	28	—	—	—	—

Note: *Significant level of *p*-value < 0.05.

model could be used to predict the efficiency of moisture vapor removal as the four factors are in the range defined in this study.

$$\text{Efficiency},\% = -50.236 - 2.086 \times T + 2.324 \times P - 0.034 \times \text{FR} + 0.045 \times T \times P - 0.017 \times P^2 - 4.346^{-5} \times \text{RH}^2 \quad (\text{adj. } R^2 = 0.947), \quad (2)$$

where T is the temperature ranging from 20°C to 45°C, P is the vacuum pressure ranging from 68 kPa to 88 kPa, RH is the initial RH ranging from 65% to 85%, and FR is the airflow rate ranging from 600 cm^3/min to 1000 cm^3/min.

The plots of the distribution of residuals in Fig 9 are used to assess the goodness of fit in regression. The scatter plot of predicted values vs actual response values (Fig 9[a]) shows that the data scattered symmetrically are close to the regressed 45° diagonal line, which indicates a good agreement between the predicted results and experimental ones. On the other hand, the normal probability plot of residuals (Fig 9[b]) is approximately linear, which proves that the error terms are normally distributed. In addition, the plot of internally studentized residuals vs predicted (Fig 9[c]) shows that the variation around the estimated regression line is uniform and there is no unusual data exceeding the upper and lower limits. As for the plot of internally studentized residuals vs run numbers (Fig 9[d]), it also proves enough accuracy of the regression model because of the random dispersion of the residues and a good distribution of experimental results (Donnelly 1984).

Verification of Regression Model

The verification test was repeated three times. The mean ± SD of the test results was 46.92 ± 2.75%, whereas the value calculated by Eq 2 is 43.69%. The experimental result is about 6.88% larger than the predicted one. It reveals that the regression model can be used to estimate the efficiency of the moisture vapor removal of the membrane system in the specified ranges of four factors.

CONCLUSIONS

In this study, a mini-scale PDMS membrane–based dehumidification system was constructed. The main effects and interactions effects of temperature, airflow rate, initial RH, and vacuum

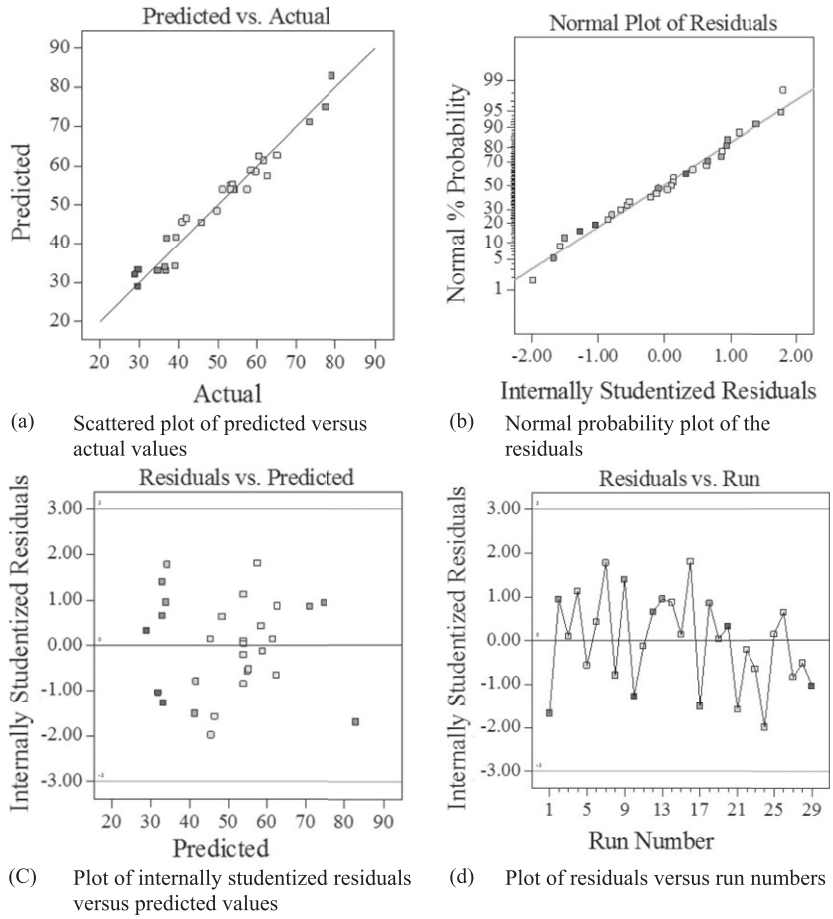

(a) Scattered plot of predicted versus actual values

(b) Normal probability plot of the residuals

(C) Plot of internally studentized residuals versus predicted values

(d) Plot of residuals versus run numbers

Figure 9. Plots of residuals in the regression analysis. (a) Scattered plot of predicted vs actual values. (b) Normal probability plot of the residuals. (c) Plot of internally studentized residuals vs predicted values. (d) Plot of residuals vs run numbers.

pressure on the efficiency of moisture vapor removal were investigated through experiments and statistical analysis. The major findings are outlined in the following texts:

1. Increasing the temperature and vacuum pressure could cause a significant increase in the efficiency of moisture vapor removal.
2. The initial RH had little influence on the efficiency of moisture vapor removal.
3. Increasing the airflow rate had a negative impact on the efficiency of moisture vapor removal.
4. The simplified regression model could be used to predict the efficiency of moisture vapor removal.

The membrane-based dehumidification system demonstrates great potential to be used in the wood-drying process and elsewhere that moisture management is a big concern, for instance, the relatively humid indoor environment in the Southern United States. The results found in this study indicate the PDMS membrane is only suitable for the low-temperature drying process. This membrane system could be used in a dehumidification kiln-drying process or as a predrying process before performing the conventional steam kiln drying. The future work of this study will address the limitations of low-temperature tolerance of the PDMS membrane to expand its application in the medium- or high-temperature drying process.

One attempt will be adding cellulose nanocrystalline to PDMS to increase the diffusion coefficient of the PDMS membrane and resistance to thermal degradation. The energy saving when applying the membrane dehumidification system will be discussed and compared with a heat pump dehumidification system in the following studies.

ACKNOWLEDGMENTS

This project was funded by the U.S. Department of Agriculture's Agricultural Research Service (USDA ARS Agreement No. 58-0204-6-003). It was also supported by the USDA National Institute of Food and Agriculture, McIntire-Stennis (Project No. ME042002) and the 2019 National Science Foundation Research Experience for Undergraduates (NSF Agreement No. 1757529).

REFERENCES

Baker RW (2012) Membrane technology and applications. Germany: John Wiley & Sons.

Bergmair D, Metz SJ, de Lange HC, van Steenhoven AA (2012) Modeling of a water vapor selective membrane unit to increase the energy efficiency of humidity harvesting. Journal of Physics: Conference Serie 395(1):012161.

Bezerra MA, Santelli RE, Oliveira EP, Villar LS, Escaleira LA (2008) Response surface methodology (RSM) as a tool for optimization in analytical chemistry. Talanta 76(5): 965-977.

Blume I, Schwering P, Mulder M, Smolders C (1991) Vapour sorption and permeation properties of poly (dimethylsiloxane) films. J Membr Sci 61:85-97.

Chadderton D (1997) Air conditioning: A practical introduction. United Kingdom: E & FN Spon.

Donnelly P (1984) Design and analysis of experiments, *in* Amer Soc Quality Control-ASQC, ASQC membership manager 611. E. Wisconsin, Montgomery, DC.

Elustondo DM, Oliveira L, Lister P (2009) Temperature drop sensor for monitoring kiln drying of lumber. Holzforschung 63(3):334-339.

Field HL, Long JM (2018) Heating, ventilation, and air conditioning. Pages 333-358 *in* Introduction to agricultural engineering technology. Germany: Springer International Publishing.

Garrahan P (2008) Drying spruce-pine-fir lumber. By FPInnovations for natural resources Canada. Special publication-SP-527E. 167 pp.

Jia L, Xu X, Zhang H, Xu J (1996) Sulfonation of polyetheretherketone and its effects on permeation behavior to nitrogen and water vapor. J Appl Polym Sci 60(8): 1231-1237.

Jia L, Xu X, Zhang H, Xu J (1997) Permeation of nitrogen and water vapor through sulfonated polyetherethersulfone membrane. J Polym Sci B Polym Phys 35(13):2133-2140.

Kneifel K, Nowak S, Albrecht W, Hilke R, Just R, Peinemann K-V (2006) Hollow fiber membrane contactor for air humidity control: Modules and membranes. J Membr Sci 276(1-2):241-251.

Liang CZ, Chung T-S (2018) Robust thin film composite PDMS/PAN hollow fiber membranes for water vapor removal from humid air and gases. Separ Purif Tech 202: 345-356.

Metz S, Van De Ven W, Mulder M, Wessling M (2005) Mixed gas water vapor/N_2 transport in poly (ethylene oxide) poly (butylene terephthalate) block copolymers. J Membr Sci 266(1-2):51-61.

Montoya, JP (2010) Using hollow fiber membranes to separate gases from liquid and gaseous streams. Pages 1-7 *in* Membrane gas exchange.

Mulder M (1996) Preparation of synthetic membranes. Pages 71-156 *in* Basic principles of membrane technology. Netherlands: Springer Netherlands. https://doi.org/10.1007/978-94-009-1766-8_3.

Park CD, Hyung CH, Kim KH, Choi WK, Park YS, Lee HK (2013) Study on the removal of water vapor using PEI/PEBAX composite hollow fiber membrane. Membr J 23(2):119-128 [in Korean].

Phillip WA, Rzayev J, Hillmyer MA, Cussler E (2006) Gas and water liquid transport through nanoporous block copolymer membranes. J Membr Sci 286(1-2):144-152

IBM SPSS Statistics for Windows, version 26.0 I Spss. 2019. New York, NY: IBM Corp.

Saldaña-Robles A, Guerra-Sánchez R, Maldonado-Rubio MI, Peralta-Hernandez JM (2014) Optimization of the operating parameters using RSM for the Fenton oxidation process and adsorption on vegetal carbon of MO solutions. J Ind Eng Chem 20(3):848-857.

Sijbesma H, Nymeijer K, van Marwijk R, Heijboer R, Potreck J, Wessling M (2008) Flue gas dehydration using polymer membranes. J Membr Sci 313(1-2):263-276.

Simpson WT (1991) Dry kiln operator's manual. United States: U.S. Department of Agriculture, Forest Service, Forest Products Laboratory.

Vildozo D, Ferronato C, Sleiman M, Chovelon J-M (2010) Photocatalytic treatment of indoor air: Optimization of 2-propanol removal using a response surface methodology (RSM). Appl Catal B 94(3-4):303-310.

Wai Lin S, Valera Lamas S (2011) Air dehydration by permeation through dimethylpolysiloxane/polysulfone membrane. J Mex Chem Soc 55(1):42-50.

Wang KL, McCray SH, Newbold DD, Cussler E (1992) Hollow fiber air drying. J Membr Sci 72(3):231-244.

Yang B, Yuan W, Gao F, Guo B (2015) A review of membrane-based air dehumidification. Indoor Built Environ 24(1):11-26.

Zhao B, Peng N, Liang C, Yong W, Chung T-S (2015) Hollow fiber membrane dehumidification device for air conditioning system. Membranes 5(4):722-738.